Live-cell imaging of endogenous Ras-GTP illustrates predominant Ras activation at the plasma membrane

Martin Augsten[1,5], Rico Pusch[2,5], Christoph Biskup[3], Knut Rennert[2], Ute Wittig[2], Katja Beyer[4], Alfred Blume[4], Reinhard Wetzker[2], Karlheinz Friedrich[1] and Ignacio Rubio[2]

[1]Institute of Biochemistry, Medical Faculty, Friedrich Schiller-University Jena, Nonnenplan 2, 07743 Jena, Germany. [2]Institute of Molecular Cell Biology, Medical Faculty, Friedrich Schiller-University Jena, Drackendorfer Str.1, 07747 Jena, Germany. [3]Institute of Physiology, Medical Faculty, Friedrich Schiller-University Jena, Teichgraben 8, 07740 Jena, Germany. [4]Institute of Physical Chemistry, Martin Luther-University, Halle-Wittenberg, Mühlpforte 1, 06108 Halle, Germany. [5]These authors contributed equally to this work.

Supplementary information

Materials and methods

Materials

Phorbol-12-myristate-13-acetate (TPA) and LPA were purchased from ICN Biomedicals and Sigma-Aldrich, respectively. EGF was a kind gift from F. D. Böhmer. Antibodies used were: Anti-pan-Ras Ab-4 from Oncogene Research

Products, anti-R-Ras (C19), anti-TC21 (V-20), anti-M-Ras (N-19), anti-GFP (FL) all from Santa Cruz Biotechnology, anti-phospho-T202/Y204- p44/42 Erk from Cell Signalling Technology, anti-CD3 (UCHT1) and anti-CD28 (CD28.2) from BD Biosciences and anti-HA hybridoma supernatant kindly provided by F. D. Böhmer. Transfection reagents polyfect, lipofectamine and DMRIE-C were from Qiagen, Invitrogen and GIBCO, respectively. Anhydrotetracycline (ATC) was purchased from Fisher Scientific. [γ-^{32}P]GTP (3000 Ci/mmol) was obtained from Hartmann Analytic. The Golgi marker BODIPY-TR-C_5-ceramide was purchased from Molecular Probes.

Cell culture, transfection, stable cell line construction

COS-7 cells were grown in DMEM supplemented with 10 % fetal calf serum (FCS) at 37°C in a 5 % CO_2 incubator. For generation of stable COS-7 clones with inducible Ha-RasS17N expression, Ha-RasS17N was appended N-terminally a myc-tag sequence and subcloned EcoRI/EcoRV into the pNRTIS-21 vector (Tenev *et al*, 2000). Neomycine resistance gene transcription is uncoupled from ATC-regulated transcription of the target gene in pNRTIS-21. pNRTIS-21/myc-Ha-RasS17N was transfected into COS-7 cells using lipofectamine according to the manufacturer's protocol. Stable transfectants were selected by supplementing the growth medium with 800 μg/ml G418 in the presence of 50 ng/ml ATC to suppress myc-Ha-RasS17N expression during the selection process. Single-cell-derived G418-resistant clones, identified by two rounds of limited dilutions, were screened for inducibility of myc-Ha-RasS17N expression upon ATC removal. In all experiments ATC was removed for a period of 48 h to induce myc-Ha-RasS17N expression. COS-7 cells and stable COS-7 clones were transfected at subconfluency with lipofectamine according to the

manufacturer´s instructions. Usually 2-3 μg total DNA were used to transfect 35 mm dishes. COS-7 cells were deprived of serum 24 h prior to experiments. COS-7 cells expressing myc-Ha-RasS17N were serum-starved 12 h in DMEM containing 0.25 % FCS.

PC12 cells were maintained in RPMI supplemented with 10 % horse serum and 5 % FCS in a 5 % CO_2 incubator. Transfection with polyfect (2 μg DNA/35 mm dish) was performed according to the manufacturer´s instructions. 24 h later cells were serum-starved for 6 h in RPMI containing 1 % horse serum and 0.5 % FCS.

Jurkat cells were maintained in RPMI supplemented with 10 % heat-inactivated FCS in a 5 % CO_2 incubator. Transfection with DMRIE-C reagent was performed with 4 μg DNA/10^6 cells according to the manufacturer´s instructions. Prior to experiments cells were serum-starved 2 h in RPMI supplemented with 50 mM HEPES (pH 7.4) and 0.2 % endotoxin-low, fatty acid-free BSA (Sigma-Aldrich).

Plasmids

The c-Raf RBD (amino acids (aa) 51-131) was amplified by PCR and cloned into pRSET B (Invitrogen) using forward primer 5´-CCG CTC GAG AAA GAC AAG CAA CAC TAT CCG T-3´ and reverse primer 5´-AAA ACT GCA GCG GAT CCC AGG AAA TCT ACT TGA AGT TC-3´encoding *Xho*I and *Pst*I sites, respectively, to yield pRSET B/RBD-1 for bacterial expression of His-tagged RBD-1. RBD-2 and RBD-3 construction involved two separate rounds of PCR amplification of RBD using primer pair 5´-AAA ACT GCA GGT AAG ACA AGC AAC ACT ATC CGT-3´ and 5´-CAT GCC ATG GCA GAT CTC AGG AAA TCT ACT TGA AGT TC-3´ encoding *Pst*I and *Nco*I sites, and primer pair 5´-CAT GCC ATG GGTAAG ACA

AGC AAC ACT ATC CG T-3´ and 5´-CCG GAA TTC TGA TCA CAG GAA ATC TAC TTG AAG TTC-3´ including *Nco*I, *Eco*RI restriction sites, respectively. PCR products were sequentially cloned on to the 3´end of RBD in pRSET B/RBD-1 to produce pRSET B/RBD-2 and –3. Primers for RBD-2 and RBD-3 were designed such that concatenated RBD-domains were separated by 5 aa linkers. R59A, R67A, T68A, N64D, K65M single point mutant RBD-1, -2 and –3 constructs were generated in the same way, starting off with the corresponding single mutant RBDs (kindly provided by C. Herrmann and A. Wittinghofer). Double point mutant RBD constructs (R59A,K65M; R59A,R67A; R59A,N64D; R59A,T68A) were constructed by site directed mutagenesis of R59A-RBD. RBD sequences were transferred from pRSET B to pEGFP-C2 (Clontech) by XhoI/EcoRI restriction cloning to yield RBD fused carboxy-terminally to enhanced green fluorescent protein (GFP). Plasmids for Ha-RasG12V, Ha-RasG12V,D38A, Ha-RasG12V,C181S,C184S, Ha-RasG12V,C186S, Ha-RasS17N, Ki-RasG12V have been described elsewhere (Rubio *et al*, 1999; Rubio *et al*, 2000). M-RasQ71L, TC21Q72L, R-RasQ78L and Rap1AG12V cDNAs were provided by Gretchen Murphy and Jean de Gunzburg, respectively. All GTPase sequences were introduced into pDsRed1-C1 (Clontech) by PCR cloning for expression of GTPase proteins in fusion with amino-terminally located DsRed1. pRSET B/Rap1GAP was donated by Jingwei Meng.

Recombinant proteins

His-tagged RBD-1, RBD-2, RBD-3, Ki-Ras, Rap1A, Rap1GAP and Ha-RasG12V proteins were expressed in *E. coli* strain BL21(De3)pLysS. Protein expression was induced in exponentially growing *E. coli* cultures by addition of 0,5 mM isopropyl-β-D-thiogalactopyranosid. 4h later bacteria were pelleted, resuspended in phosphate

buffered saline containing 1% Triton X-100, 5 mM $MgCl_2$ and protease inhibitors, and cells were broken by three freeze/thaw cycles. The sample was sonicated with a Branson tip sonicator (five cycles, each 15 s on ice) and centrifuged at 30000 rpm and 4°C for 30 min. The cleared supernatant was loaded on a Hi-Trap Chelating HP column (AmershamPharmacia) preloaded with Ni^{2+}. His-tagged proteins were eluted over an imidazol gradient and protein rich fractions were collected and concentrated over a 10-kDa cut-off membrane. The protein sample was dialysed against 25 mM Tris/HCl (pH 7.5), 200 mM NaCl, 5mM $MgCl_2$. Protein concentration was determined by the Bradford assay. Purity of all preparations was higher than 90 %. GST-NF-1cat was purified from bacteria by glutathione affinity chromatography as previously described (Rubio *et al*, 1999) and stored at - 20ºC in 25 mM HEPES (pH 7.5), 50 % glycerol.

GAP protection assays

Assays were performed essentially as described (Rubio *et al*, 1999). Briefly, 1 μg His-Ki-Ras or 10 μg His-Rap1A protein was loaded with [γ-^{32}P]GTP in 25 μl (final volume) of 25 mM HEPES (pH 7.5), 50 mM NaCl, 10 mM EDTA, 2 mg/ml BSA, 0.1 % Triton X-100, 130 nM [γ-^{32}P]GTP. The sample was diluted to 500 μl with ice cold 25 mM HEPES (pH 7.5), 5 mM $MgCl_2$, 0.1 % Triton X-100, kept 5 min on ice, and made 400 μM in GTP. The mixture was split, supplemented with RBD proteins as applicable and kept on ice for further 5 min. GAP reactions were started by addition of 0.5-1.8 μM final concentration GST-NF-1cat (catalytic domain of the Ras-GAP NF-1, aa 1172-1538, in fusion with GST) or 50 nM Rap1GAP (volume added never exceeded 5 % of total sample volume) and putting the tubes to 30°C. At the indicated

time points, 20 µl of the reaction were transferred to tubes containing 480 µl ice cold 5 % activated charcoal in 7.5 mM phosphoric acid (pH 2.5) and thoroughly vortexed. After 15 min on ice, the samples were centrifuged at 20000g, 4°C for 15 min. 200 µl of the supernatant containing anorganic [γ-^{32}P]phosphate were subjected to Cerenkov counting.

Isothermal titration calorimetry

300 µM His-tagged Ha-RasG12V in 25 mM Tris/HCl (pH 7.5), 200 mM NaCl, 5 mM EDTA, 10 mM GTP (sodium salt) was incubated 5 min at 37°C, made up to 20 mM $MgCl_2$, and concentrated over a 10-kDa cut-off membrane. Free GTP was separated from Ras-GTP complexes by gel filtration (Sephadex G25; AmershamPharmacia) in 25 mM Tris/HCl (pH 7.5), 200 mM NaCl, 5 mM $MgCl_2$. The amount of GTP-loaded Ha-RasG12V in the final sample routinely amounted to 90-95 %, as determined by HPLC analysis of Ras-bound GTP and GDP. ITC was performed essentially as described by Rudolph *et al* (Rudolph *et al*, 2001), except for the proteins used (His-tagged proteins, Ha-RasG12V-GTP instead of Ha-Ras in its guanosine 5´-(β,γ-imido)triphosphate form) and a buffer of different composition. Briefly, the temperature-controlled mess chamber of an isothermal titration calorimeter (VP-ITC, Microcal^{TM} Inc.) was filled with 20 µM His-RBD-1, 10 µM His-RBD-2 or 6,7 µM His-RBD-3 in 25 mM Tris/HCl (pH 7.5), 200 mM NaCl, 5mM $MgCl_2$ and the syringe with His-Ha-RasG12V-GTP at 20-30fold higher concentration in the same solution. In each computer-controlled injection step 1 to 7 µl of Ras were titrated to the RBD and the change in heating power was measured until saturation was reached, indicated by constant power pulses. This heat background was virtually identical to that

obtained in control experiments titrating Ras against buffer. Integrated pulses were corrected for these background values, and the data were analysed using Origin 5.0 (Microcal^{TM}, Inc) yielding stoichiometry (*N*; in the current case reflecting Ras-GTP/RBD binding valency), the binary equilibrium association constant K_a, and the enthalpy of binding ΔH. From $\Delta G° = \Delta H° - T\Delta S°$ and $\Delta G° = -RT \ln K_a$, the free energy of binding $\Delta G°$ and the entropy $\Delta S°$ were calculated. The data were averaged over three independent experiments.

Confocal imaging

COS-7 and PC12 cells were grown either on glass coverslips or in glass bottom dishes (a kind gift from MatTek Corporation or, alternatively, custom made using gridded cover slips from Eppendorf) coated with collagen. Cells were transfected and serum-starved as described above. 45 min prior to imaging cells were treated with the Golgi tracker BODIPY-TR-C_5-ceramide acording to the manufacturers´instructions. In the final wash step medium was replaced for fresh starvation medium buffered with 25 mM HEPES (pH 7.4). Jurkat cells were plated on poly-L-lysine-coated glass bottom dishes 10 min prior to imaging.

Confocal images were acquired with a Zeiss LSM 510 (Carl Zeiss GmbH, Oberkochen, Germany) inverted laser scanning microscope using a C-Apochromat 63x water immersion objective lens (Zeiss). Cells were imaged at room temperature or at 37°C using a thermostated chamber with indistinguishable results. GFP and DsRed/BODIPY-TR-C_5-ceramide were excited with the Ar 488 nm and the HeNe 543 nm laser lines, respectively. GFP fluorescence was recorded with a 505-550 nm band-pass filter (‘green channel’). A 560 nm long-pass filter was used to record the

BODIPY-TR-C_5-ceramide fluorescence ('red channel'). The confocal aperture was adjusted to give optical sections of 0.8 μm (Jurkat) or 1 μm (COS-7 and PC12 cells). Before growth factor administration cells were monitored for at least five minutes. Cells with low and uniform cytosolic fluorescence intensity were preferentially chosen for visualisation of endogenous Ras-GTP. Images were captured at set time intervals for a period of at least 30 minutes after stimulation. LSM image files were processed using the Zeiss LSM image browser software (Version 3.1).

Fluorescence quantification

Fluorescence signals recorded from the probe were low for several reasons: (1) Probe expression levels were low. Since endogenous Ras-GTP levels are low, probe expression levels had to be at least in the same order of magnitude to ensure that a sufficiently high fraction of reporter molecules re-distributed within the cell.

(2) To minimize photobleaching, low excitation powers and reasonably short acquisition times had to be chosen. (3) To observe the re-distribution of the probe in a small optical section (0.8-1.0 μm), a small confocal aperture had to be chosen. (4) To ensure a high signal to noise ratio, which is a prerequisite for quantifying fluorescence signals, a sub-maximal detector voltage had to be used.

All these factors resulted in fluorescence images, in which pixel intensities were too low to allow a quantification of probe fluorescence in the conventional way of using rectangular ROIs: Slight increases in fluorescence intensity originating from the plasma membrane are cancelled out by surrounding regions so that the average fluorescence intensity of a rectangular ROI at the plasma membrane is not significantly higher than the ROI in cytosolic regions.

To circumvent this problem and to reliably detect slight regional changes in fluorescence intensity we have programmed an automatic cell image segmentation algorithm that yielded masks for four cellular regions: the plasma membrane, the Golgi apparatus, the cytosol and the nucleus. The Golgi compartment was identified by the fluorescence signal of the Golgi tracker BODIPY-TR-C_5-ceramide. GFP fluorescence was used to distinguish plasma membrane (PM) and nucleus from the cytosol (see Supplementary Fig. 8 online for details). Based on the masks, mean fluorescence intensities were calculated for the PM, Golgi and the cytoplasm. The nuclear and immediate perinuclear region were excluded from the analysis. PM/cytoplasma and Golgi/cytoplasma ratios were calculated for a series of images and plotted as a function of time (Figure 4 B and Figure 5 C). All data are presented as normalized mean values (± SEM).

Ras-GTP pull-down and Erk activation assays

Ras-GTP levels were determined using the c-Raf RBD protein in fusion with GST to pull out active Ras-GTP complexes from cell extracts. COS-7 and stably transfected COS-7 cells were seeded in 6-well plates, serum-starved at subconfluency and challenged as appropriate. Cells were lysed and extracts processed exactly as described (Rubio *et al*, 2000). Pull-down assays for detection of active R-Ras, TC21 and M-Ras were carried out in exactly the same way. Serum-starved Jurkat cells were aliquoted at 10^6cells/0.5 ml in RPMI containing 50 mM HEPES (pH 7.4) and 0.2 % endotoxin-low, fatty acid-free BSA. Following stimulation cells were spun down quickly, the supernatant was aspirated and cell pellets were lysed and processed as described for COS-7 cells. For determination of Erk activity COS-7 cells were transfected with HA-tagged Erk2 in combination with other cDNAs as described

above. Cells were lysed in ice-cold 50 mM Tris/HCl (pH 7.5), 150 mM NaCl, 5 mM EDTA, 1 % NP-40, protease inhibitors, phosphatase inhibitors. An aliquot of the cleared cell extract was analysed by Western blotting with anti-phospho-T202/Y204-Erk antibody, which decorates active Erk, and membranes were reblotted for total Erk levels with anti-HA antibody.

Supplementary references

Rubio I, Wittig U, Meyer C, Heinze R, Kadereit D, Waldmann H, Downward J, Wetzker R (1999) Farnesylation of Ras is important for the interaction with phosphoinositide 3-kinase γ. *Eur J Biochem* **266**: 70-82

Rubio I, Wetzker R (2000) A permissive function of phosphoinositide 3-kinase in Ras activation mediated by inhibition of GTPase-activating proteins. *Curr Biol* **10**: 1225-1228

Rudolph MG, Linnemann T, Grunewald P, Wittinghofer A, Vetter IR, Herrrmann C (2001) Thermodynamics of Ras/effector and Cdc42/effector interactions probed by isothermal titration calorimetry. *J Biol Chem* **276**: 23914-23921

Tenev T, Boehmer SA, Kaufmann R, Frese S, Bittorf T, Beckers T, Boehmer FD (2000) Perinuclear localization of the protein-tyrosine phosphatase SHP-1 and inhibition of epidermal growth factor-stimulated STAT1/3 activation in A431 cells. *Eur J Cell Biol* **79**: 261-271

A

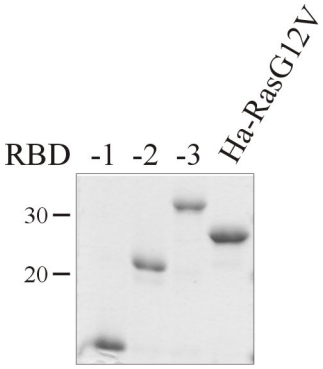

B

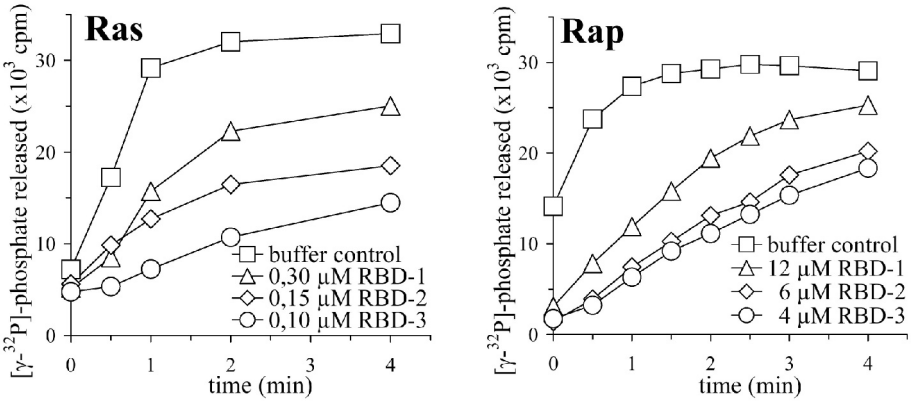

C

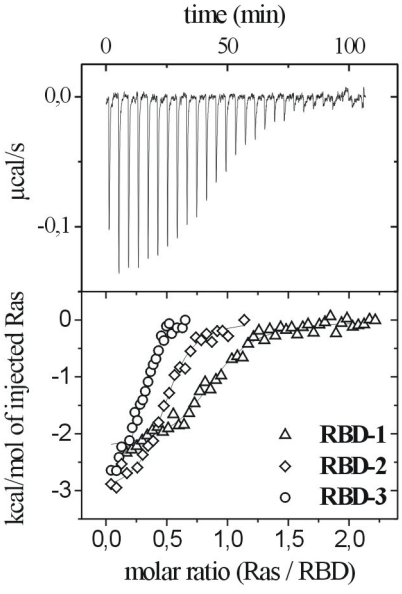

D

	RBD-1	RBD-2	RBD-3
N	0,93 +/- 0,05	0,59 +/- 0,05	0,35 +/- 0,03
Ka	5,86 +/- 1,72	16,23 +/- 3,98	18,53 +/- 3,00
ΔH^o	-2221 +/- 78	-2942 +/- 64	-2997 +/- 79
ΔS^o	18,67 +/- 0,52	18,42 +/- 0,49	18,58 +/- 0,58

Supplementary Figure 1

In vitro characterization of RBD/Ras interactions. (A) Recombinant His-tagged RBD-1, RBD-2, RBD-3 and Ha-Ras proteins produced in E. coli. (B) GAP protection assays. Left panel: Ras/GAP assay, right panel: Rap/GAP assay. [α-^{32}P]GTP-loaded Ras/Rap protein was incubated with buffer control or indicated concentrations of RBD-1/2/3. Reactions were initiated by addition of the Ras-GAP NF-1 or Rap1GAP, respectively. (C) ITC analysis of Ras-GTP/RBD-1/2/3 interactions. Upper panel: representative raw data acquisition for the RBD-1/Ha-RasG12V pair. Lower panel: representative curves of integrated heat values for all three pairs. Lower x-axis unit is defined as molar ratio of Ras-GTP/RBD valency. (D) Summary of thermodynamic parameters and stoichiometry of Ras-GTP/RBD-1, -2, and -3 interactions obtained from three independent ITC measurements. His-tagged Ha-RasG12V produced in bacteria to 95 % purity (see A) was loaded with GTP and titrated to 20 µM RBD-1, 10 µM RBD-2 or 6,7 µM RBD-3. Ka is given in 10^5 M^{-1}, ΔH^o in cal/mol and ΔS^o in cal/mol/K. N: Ras/RBD binding equivalent stoichiometry, reflects the ratio Ras-GTP/RBD binding valency in RBD-1, -2 and -3. The Ka value for the RBD-1/Ras-GTP interaction obtained here differs substantially from previous determinations (Rudolph et al, 2001). We suspect this discrepancy to be related to differences in our experimental setup. Notwithstanding the deviation in the absolute figures, these data evidence that oligomerization of RBD results in stronger binding to Ras-GTP with one-to-one stoichiometry.

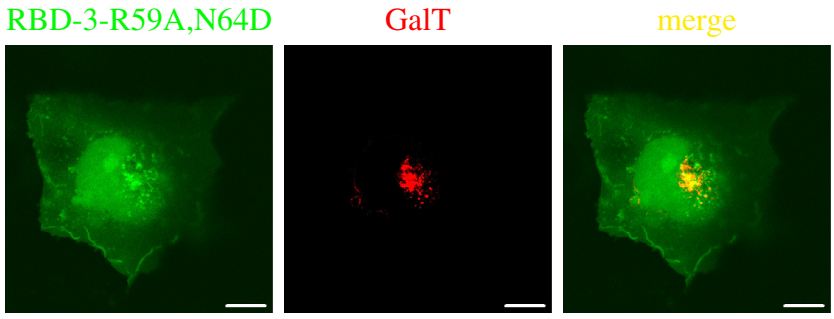

Supplementary Figure 2
Overexpressed Ha-RasG12V recruits GFP-RBD-3-R59A,N64D to the Golgi. COS-7 cells were transfected with Ha-RasG12V, GFP-RBD-3-R59A,N64D and the Golgi marker Galactosyl transferase (GalT) coupled to DsRed. Cells were imaged confocally. Bars: 10 µm.

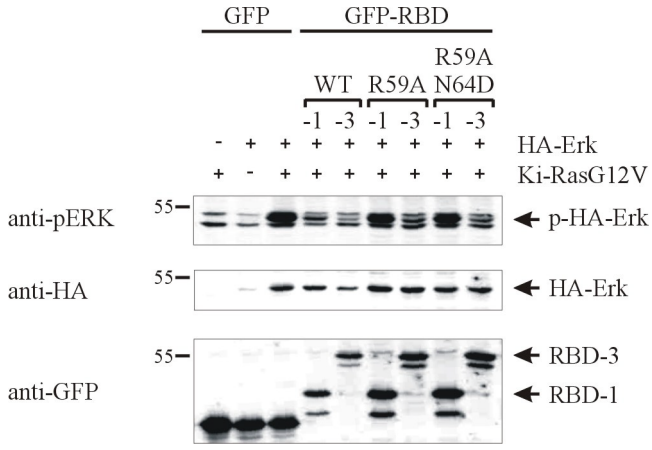

Supplementary Figure 3
RBD proteins attenuate Ras signalling in an oligomerization-dependent manner. COS-7 cells were transfected with Ki-RasG12V and HA-Erk in combination with GFP or indicated GFP-RBD variants. 48 h later cells were lysed and analysed by Western blotting for Erk phosphorylation/activation and heterologous protein expression using antibodies indicated on the left side of the panel.

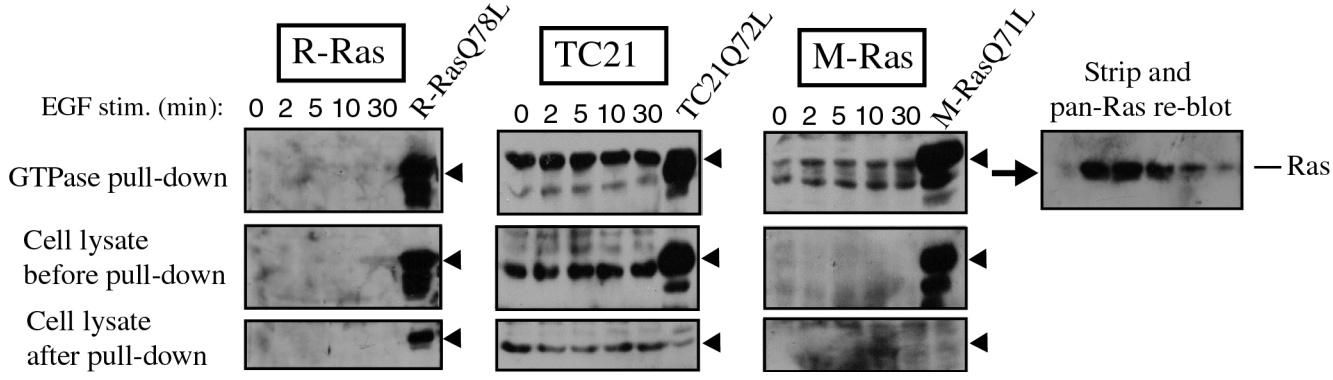

Supplementary Figure 4
Lack of EGF-induced R-Ras, TC21, M-Ras activation. Serum-starved COS-7 cells were stimulated for the indicated time periods with 50 ng/ml EGF and subjected to a Raf-RBD pull-down as described in the experimental section. Samples from individual experiments were processed in Western blots for R-Ras, TC21 and M-Ras. Experiments included one transfection with untagged constitutively-active R-RasQ78L, TC21Q72L or M-RasQ71L, respectively. Each panel features as a loading control cell extract samples taken before and after the affinity precipitation. The pull-down membrane of the M-Ras experiment was re-probed with pan-Ras antibody against Ha-, Ki, and N-Ras to validate the functionality of the assay. Arrowheads mark migration of the 26 kD molecular size marker.

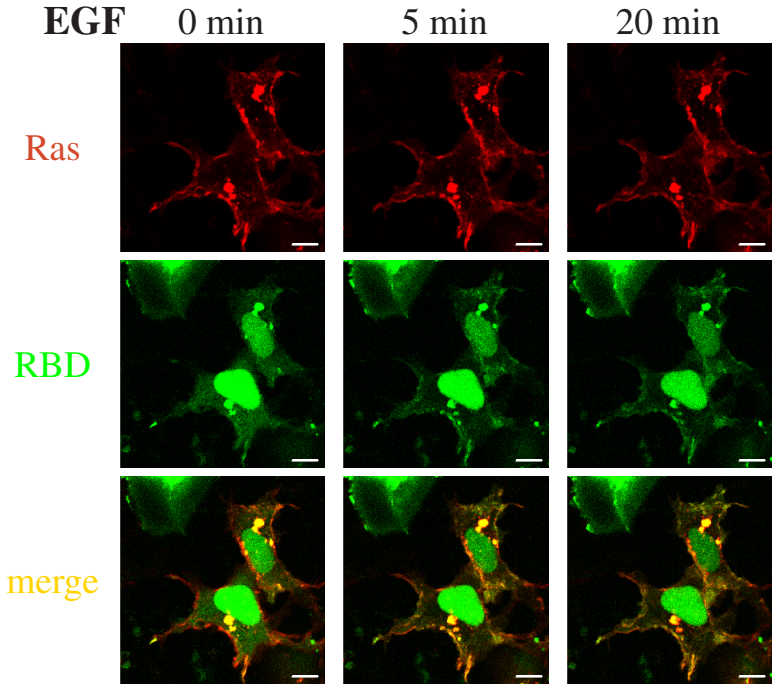

Supplementary Figure 5
Ras overexpression accentuates agonist-induced GFP-RBD-3-R59A,N64D translocation to the PM. COS-7 cells were co-transfected with DsRed-Ha-Ras and GFP-RBD-3-R59A,N64D. Cells were deprived of serum, exposed to 50 ng/ml EGF and imaged confocally. Remarkably, around 50 % of serum-deprived cells featured perinuclear co-localisation of overexpressed DsRed-Ras and GFP-RBD-3-R59A,N64D. This perinuclear signal did not change upon EGF or LPA (data not shown) stimulation, indicating that perinuclear Ras-GTP, as reported by GFP-RBD-3-R59A,N64D, was not under the control of growth factor-elicited signals.
Bars: 10 μm.

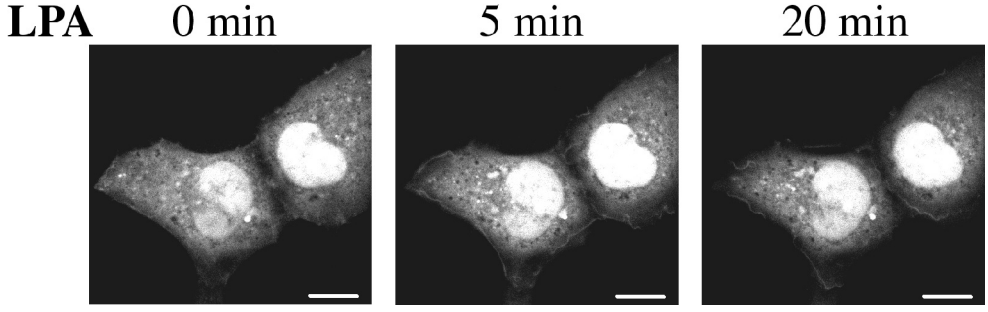

Supplementary Figure 6
Lysophosphatidic acid promotes probe re-distribution to the PM in the absence of membrane ruffling. COS-7 cells transfected with GFP-RBD-3-R59A,N64D were deprived of serum and challenged with 10 μM LPA. Confocal pictures were taken at the indicated time points. Bars: 10 μm.

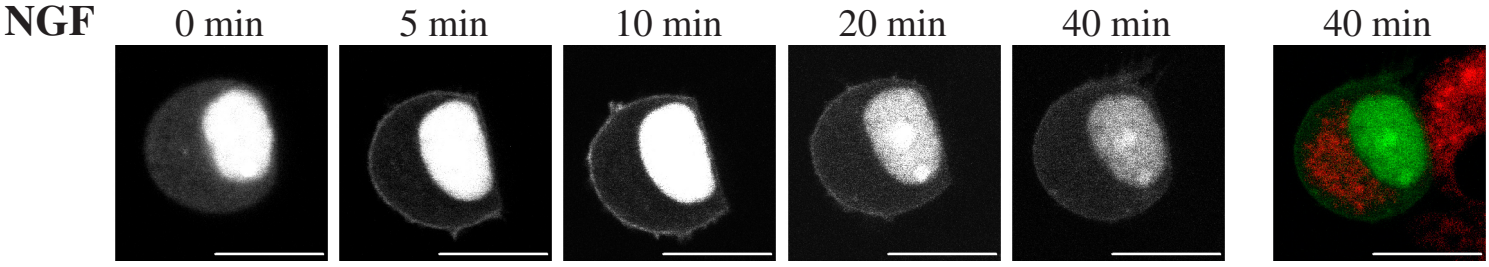

Supplementary Figure 7
Ras overexpression increases NGF-induced GFP-RBD-3 re-distribution to the PM in PC12 cells. Serum-starved PC12 cells co-expressing Ha-Ras and GFP-RBD-3 were stained with the Golgi marker BODIPY-TR-C5-ceramide, challenged with NGF and imaged alive. Note that Ha-ras overexpression results in a shlightly slower attainment of maximum PM illumination compared to endogenous Ras (Figure 4A). White and green: GFP-RBD-3; Red: BODIPY-TR-C5-ceramide. Bars: 10 μm.

A Original contrast enhanced laser scanning image

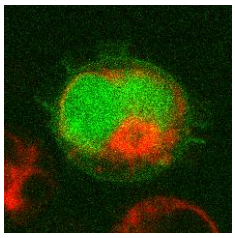

B Green and red channel of the LSM image

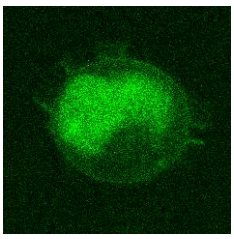

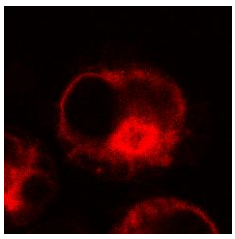

C Filtered, contrast enhanced image

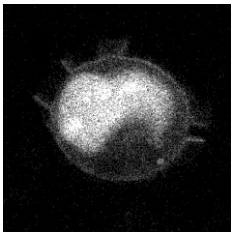

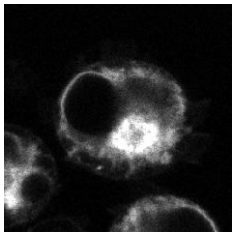

D Gradient image

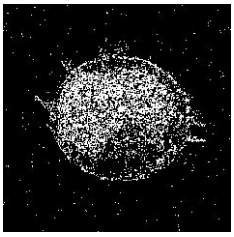

E Final masks

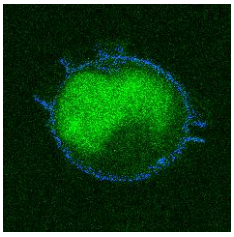

Plasma membrane

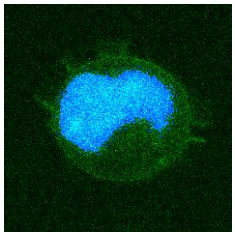

Cell nucleus

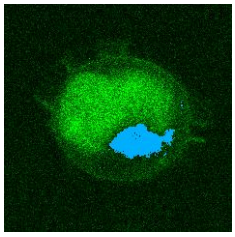

Golgi

F Segmented Image

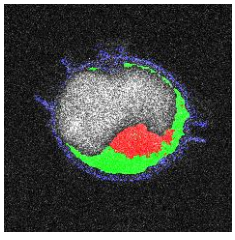

Supplementary Figure 8

Major steps of the automated segmentation process. (A) Original contrast enhanced image of a Jurkat cell. (B) Green and Red channel of the original image. The green channel was used to record GFP fluorescence, whereas BODIPY-TR-C_5-ceramide fluorescence was recorded in the red channel (see Supplementary Methods for details). (C) Filtered image. To reduce noise but to preserve edges images were filtered by a two-dimensional order-statistic filtering algorithm. (D) Gradient image. Strong edges were detected by identifying pixels where the gradient of the filtered image was steepest. Weak edges were only included in the mask if they were connected to strong edges. In this way the algorithm was robust enough not to be fooled by noise while it was still able to detect small intensity changes between the cell and the background. (E) Masks for the plasma membrane, nucleus and Golgi apparatus. The gradient images were used to create the masks for the plasma membrane and the nucleus. The Golgi apparatus was identified by selecting pixels that were above a set intensity threshold in the red channel. Because of the high intensity differences between nucleus and the surrounding cytosol this approach could also be used to identify the nuclear region yielding the same result as the gradient method, but it was ineffective in identifying the plasma membrane. (F) Segmentation result. Regions of the plasma membrane and the Golgi that were overlapping with the nucleus were not evaluated. Pixel intensities in the marked regions were averaged and used to calculate the plasma membrane/cytosol or Golgi/cytosol ratios plotted in Figure 4B and 5C (see Supplementary Methods for details).